Scientific Research Publishing

Open Journal of Applied Sciences, 2024, 14, 3731-3747
https://www.scirp.org/journal/ojapps
ISSN Online: 2165-3925
ISSN Print: 2165-3917

A Modularizable High-Frequency Battery Equalizer with Multi-Winding Transformer for Energy Storage Systems

Chihchiang Hua[1], Jianbin Lai[2], Zhewei Zhang[1]

[1]Department of Electrical Engineering, National Yunlin University of Science and Technology, Yunlin
[2]Graduate School of Engineering Science and Technology, National Yunlin University of Science and Technology, Yunlin
Email: huacc@yuntech.edu.tw, D11210206@yuntech.edu.tw, M11012054@yuntech.edu.tw

How to cite this paper: Hua, C.C., Lai, J.B. and Zhang, Z.W. (2024) A Modularizable High-Frequency Battery Equalizer with Multi-Winding Transformer for Energy Storage Systems. *Open Journal of Applied Sciences*, **14**, 3731-3747.
https://doi.org/10.4236/ojapps.2024.1412243

Received: November 18, 2024
Accepted: December 28, 2024
Published: December 31, 2024

Abstract

This paper proposes an improved modularizable high-frequency battery equalizer with multi-winding transformer for energy storage systems. The involvement of parasitic components in circuit resonance, along with the addition of a resonant network, enables soft-switching for the power switches to reduce the switch voltage stress due to high frequency switching operation. The proposed circuit is designed to operate at switching frequency of 1 MHz. The detailed analysis of circuit operation is provided. At last, the feasibility and performance of the proposed battery equalizer are demonstrated through the system implementation and experimental tests of a prototype circuit. Experimental results have shown zero voltage switching (ZVS) is achieved on the switches.

Keywords

Battery Equalizer, High Switching Frequency, Multi-Winding Transformer

1. Introduction

Due to abnormal climate changes, countries worldwide have begun to focus on climate change issues. To reduce greenhouse gas emissions, renewable energy and electric vehicles have become key areas of concern. However, due to the instability of renewable energy, energy storage systems are needed as complements in lots of applications. The primary power source for electric vehicles is battery system. In battery applications, such as lithium iron phosphate single cells, with voltages typically ranging only from 2 to 4.3 V, they need to be connected in series to achieve the required voltage for electric vehicles or energy storage systems. However, individual cells in a series-connected battery pack may experience mismatch issues

due to manufacturing errors, battery aging during use, and other factors. This mismatch can lead to the "bucket effect," causing a decrease in the overall capacity of the battery pack and affecting its lifespan. In the worst-case scenario, it may result in overcharging, leading to accidents such as explosions or fires. Therefore, the use of a battery equalizer is necessary to balance individual cells within the battery pack, and there has been significant research on battery equalizers over the years. Technologies related to charge equalization are continually being explored and actively developed [1]-[11].

The simplest structure for dissipative equalization is to parallel resistors with the same resistance value for each battery cell unit, maintaining the same terminal voltage for each battery unit. The drawback of this approach is that the energy of the batteries is dissipated in the form of heat through the resistors, reducing the available energy and causing a significant temperature rise on the resistors [12]-[16]. To reduce energy losses in batteries, resistive components can be replaced with zener diodes because energy balancing only occurs when the zener diodes undergo reverse breakdown. This effectively reduces the energy loss in the batteries. However, this structure can only prevent overcharging and does not address the issue of overdischarging [16].

To mitigate the continuous losses brought by the resistive dissipative equalization structure, an active-switch-based resistive dissipative equalization structure has been developed [16]. Its control strategy is more flexible than the zener diode equalization structure, but it requires more feedback detectors, making the implementation of the energy balancing control strategy more complex.

Due to the significant energy losses in the analyzed dissipative equalization structures, the development of an efficient non-dissipative equalization structure becomes crucial. The non-dissipative equalization structure is based on the concept of energy transfer and can effectively reduce energy losses in batteries.

Switched capacitor equalization is a method that operates by high-frequency switching, temporarily storing energy from battery cells with higher charge in capacitors, and then transferring it to cells with lower charge to achieve equalization [13] [17] [18]. This equalization method has simple control and does not require circuit detection for feedback control. However, the energy transfer occurs through extremely high-pulse currents, and the equalization time is closely related to capacitor capacity, potential difference between batteries, and switching frequency, leading to potential issues of prolonged equalization time. The global buck-boost converter equalization structure works by evenly distributing the energy of battery cells with higher charge to other cells, reducing the complexity of control strategy. However, it can only provide real-time protection for batteries with high charge, preventing overcharging, and cannot offer immediate protection for the battery with the lowest charge [19]. The adjacent buck-boost converter equalization structure can only balance neighboring battery cells. While it can provide real-time protection for the battery with the lowest charge, it cannot uniformly distribute energy throughout the battery pack, leading to longer equaliza-

tion time [14]. The bidirectional adjacent buck-boost converter equalization structure is an improved version of the adjacent structure and can more effectively distribute energy among individual cells. However, its drawback is the increased complexity of control strategies [14] [20].

The multi-winding flyback converter equalization topology is based on the concept of Faraday's law of electromagnetic induction windings with the same number of turns can induce the same electromotive force, reducing the number of detection units and the complexity of system control. However, the volume of the transformer core in the flyback circuit is closely related to the performance of battery equalization, making this topology not suitable for a large series-connected battery packs. The secondary multi-winding flyback converter equalization structure distributes the total energy of the battery pack to cells with lower energy to prevent over-discharge during battery discharging interval. It is suitable for discharge scenarios because the system has only one active switch, simplifying the control strategy [13] [21]-[23]. The primary multi-winding flyback converter equalization system releases the energy of the battery cells to be overcharged and returns it to the battery pack to prevent overcharging of the specific cell. It is suitable for the charging process of the battery pack [15] [24]. To address the limitation of applying the multi-winding flyback converter to a large number of batteries, a modular design is adopted in [25] to reduce the transformer volume and enhance flexibility. The multi-flyback converter equalization system uses a separate flyback converter for each battery cell to evenly distribute voltage and current stress. However, the drawback is that the circuit cost is quite high [12] [15].

The multi-winding transformer equalization system is similar to the multi-winding flyback converter system, with the difference that the transformer in the multi-winding transformer equalization system is used to transmit energy rather than store it. When the transformer operates in bidirectional mode, it can increase the power density of the transformer, making it suitable for high-voltage and high-power applications.

The half-bridge multi-winding transformer equalization system in [1] [16] [26] operates with a duty cycle of fifty percent for each of the two active switches, exhibiting zero voltage switching (ZVS) characteristics during turn-on to reduce switching losses of the switches. The rectifying diodes exhibit zero current switching (ZCS) during turn-off. On the other hand, due to the presence of two forward voltage drops across diodes in each rectification path of the secondary-side bridge rectifier, this bridge rectifier introduces higher power loss in low-voltage output scenarios. In other words, when the load corresponding to the secondary winding of the multi-winding transformer equalization system is a single battery cell, a bridge rectifier may not be suitable as the secondary-side rectification system.

Applying the E-class converter to the multi-winding transformer equalization system provides the advantages of flexible switching, reduction of switching losses and electromagnetic interference on the switches [27]. Because this topology in-

volves only one active switch, it significantly simplifies circuit topology and control for the system. However, due to the high voltage and current stresses on the active switch, the E-class converter is not suitable for applications in high-voltage/high-power scenarios, such as electric motorcycles. On the other hand, using a full-wave voltage multiplier as the rectification scheme can reduce the number of transformer secondary windings by half compared to a bridge rectifier scheme. Additionally, this scheme has only one diode per rectification path, reducing the forward voltage drop by half [27]-[29].

The selective isolated converter equalization system features only one isolated converter, significantly reducing the complexity of the equalization circuit [1] [26]. Because this topology uses only one isolated converter, there is no problem of mismatch between multiple converters or multi-winding transformers. However, the control strategy for the selection switches must be extremely rigorous to avoid irreversible damage to the batteries, as simultaneous conduction of the selection switches corresponding to each battery cell would lead to a short circuit.

Since the adoption of a lot of batteries in a battery energy system is becoming a trend, a high-frequency multi-winding transformer battery equalizer is proposed in this paper. The proposed converter is based on the advancements presented in [23] and incorporates the principles of high-frequency circuit design [30] [31]. Increasing the switching frequency enhances the power density of the equalizer, effectively minimizing the circuit volume. Furthermore, the adoption of a modular design enhances versatility of the system.

2. Proposed Battery Equalizer

2.1. Proposed Circuit

A high-frequency battery equalizer with multi-winding transformer for battery energy systems is proposed as shown in **Figure 1**. In the proposed converter, the L_r-C_r network in parallel on both sides of the switch is connected to reduce the impedance of the second-order harmonic, which increasing the impedance of the third-order harmonic in the off state. Consequently, the voltage on the switch can be expressed as the sum of the first-order harmonic and the third-order harmonic, resulting in a quasi-trapezoidal waveform, as shown in **Figure 2** [32].

The terms used for the proposed equalizer are defined as follows:

i is the module number.

j is winding number.

V_{Bij} is the voltage of battery B_{ij}.

L_{ij} is the winding leakage inductance.

T_{ij} is the winding number.

S_{ij} is the switching number.

C_{sij} is the switch parasitic capacitance.

C_{rij} Resonant Network Capacitance.

L_{rij} Resonant Network inductance.

L_m is the magnetizing inductance.

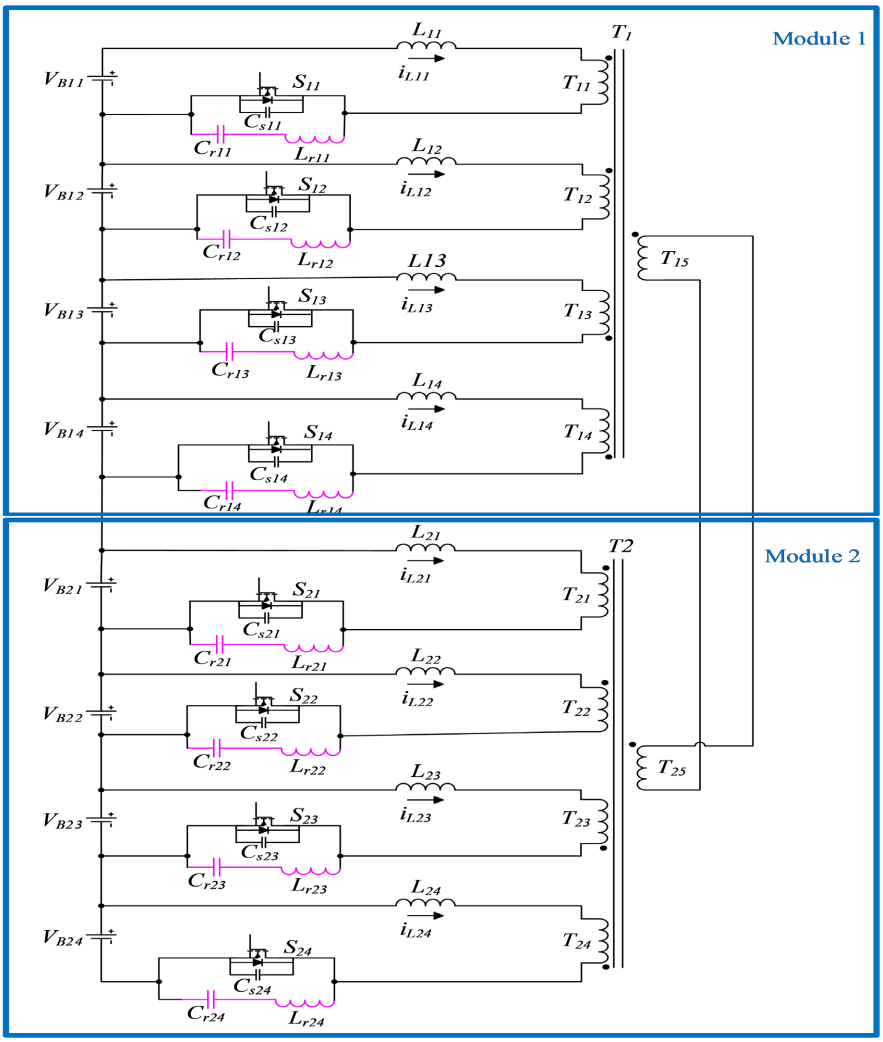

Figure 1. The proposed high frequency equalizer with multi-winding transformer.

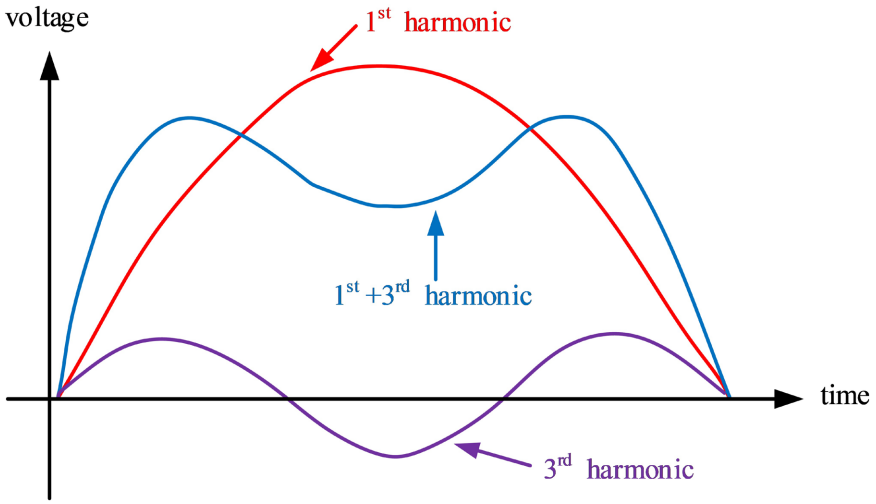

Figure 2. Half-wave quasi-trapezoidal waveform.

2.2. Equilibrium Mode of Operation Analysis

To simplify the circuit analysis, a single module is examined for the proposed system, as shown in Figure 3. Since each module is identical, the analysis of operation for a single module is provided. The circuit adopts symmetrical pulse width modulation (PWM), leading to two distinct modes in its operation. For the analysis of operation, $V_{B1} > V_{B2} > V_{B3} > V_{B4}$ is assumed.

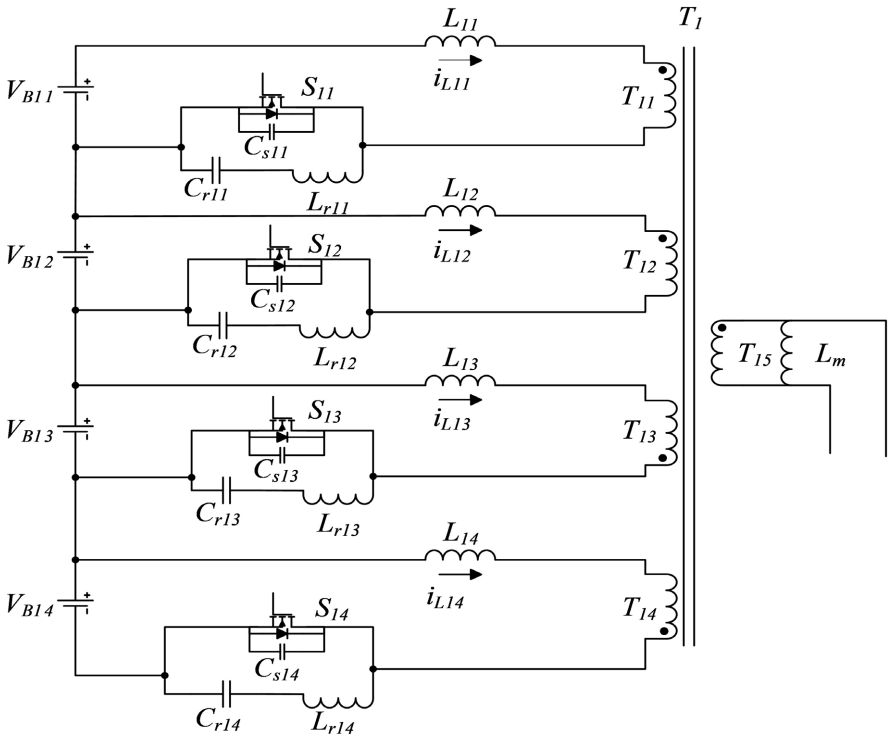

Figure 3. The simplified battery equalization circuit.

Mode I(t_0-t_1): During this mode, as shown in Figure 4(a), the switch for the positive half cycle is activated. In this configuration, the two loops associated with V_{B1} and V_{B2} facilitate charge equalization in the forward direction, effectively transferring the energy from the high-voltage battery in the magnetizing inductance L_m. The voltage across the winding during this mode can be represented as follows:

$$V_{T11} = V_{T12} = V_{T1}(t) = \frac{1}{2}\sum_{a=1}^{2} V_{Ba},\ 0 < t < \frac{T}{2}. \tag{1}$$

The charging current of the battery is

$$\begin{cases} i_{B11}(t) = i_{B11}(t_0) + \dfrac{V_{B11} - V_{T11}}{L_{11} + L_m}(t_1 - t_0) \\ i_{B12}(t) = i_{B12}(t_0) + \dfrac{V_{B12} - V_{T12}}{L_{12} + L_m}(t_1 - t_0) \end{cases},\ 0 < t < \frac{T}{2}. \tag{2}$$

From (2), if the battery current is positive, the battery is discharging, otherwise, the battery is charging. The magnetizing current i_{Lm} is

$$i_{Lm}(t)=\left\{i_{B11}(t)+i_{B12}(t)\right\}\cdot N_{T1},\ 0<t<\frac{T}{2}. \tag{3}$$

where N_{T1} is the turns ratio of transformer T_1

$$N_{T1}=\frac{N_{T11}}{N_{T15}}=\frac{N_{T12}}{N_{T15}}. \tag{4}$$

Mode II(t_1-t_2): In the mode shown in Figure 4(b), the negative half cycle is activated. During this mode, the two loops corresponding to V_{B3} and V_{B4} are engaged, facilitating forward equalization for both loops. Simultaneously, the energy stored in the magnetizing inductance L_m is released to the low-voltage battery through the flyback operation, completing the transformer reset.

$$V_{T13}=V_{T14}=V_{T1}(t)=\frac{1}{2}\sum_{b=3}^{4}V_{Bb},\ \frac{T}{2}<t<T. \tag{5}$$

The charging current of the battery is

$$\begin{cases} i_{B13}(t)=i_{B13}(t_1)+\dfrac{V_{B13}-V_{T13}}{L_{13}+L_m}(t_2-t_1) \\ i_{B14}(t)=i_{B14}(t_1)+\dfrac{V_{B14}-V_{T14}}{L_{14}+L_m}(t_2-t_1) \end{cases},\ \frac{T}{2}<t<T \tag{6}$$

Hence, the magnetizing current i_{Lm} is

$$i_{Lm}(t)=\left\{i_{B13}(t)+i_{B14}(t)\right\}\cdot N_{T2},\ \frac{T}{2}<t<T. \tag{7}$$

where N_{T2} is the turns ratio of transformer T_2

$$N_{T2}=\frac{N_{T13}}{N_{T15}}=\frac{N_{T14}}{N_{T15}}. \tag{8}$$

From Equations (3) and (7), it is obvious that energy transfer occurs through the magnetizing inductance of the transformer during the equalization process between positive and negative half cycles. Equations (2) and (6) reveal that forward equilibrium is adopted during both the positive and negative half cycles.

2.3. Bi-Directional Resonant Mode Analysis

The proposed converter incorporates parasitic components into resonance by integrating them into the L_r-C_r network, as illustrated in Figure 5. Similar to the equalization mode, bidirectional resonance occurs in both modes. The parasitic components include transformer leakage inductance (L_{ij}), switch parasitic capacitance (C_{sij}), and the elements L_{rij} and C_{rij} of the resonant network. The circuit is simplified and the operation analysis is given.

Mode I(t_0-t_1): During this mode, switch S_{11} is turned on, and S_{13} is turned off. Components L_{11}, L_{13}, C_{S13}, and the resonant network L_{r13}-C_{r13} engage in resonance. The resonance involving C_{S13} ends when V_{CS13} drops to zero.

Mode II(t_1-t_2): In this mode, L_{r13} and C_{r13} ensure ZVS for the activation of switch S_{13}. Simultaneously, switch S_{11} is turned off, and components L_{11}, L_{13}, C_{S11}, L_{r11}, and C_{r11} participate in resonance during this mode. Similar to Mode I, the resonance

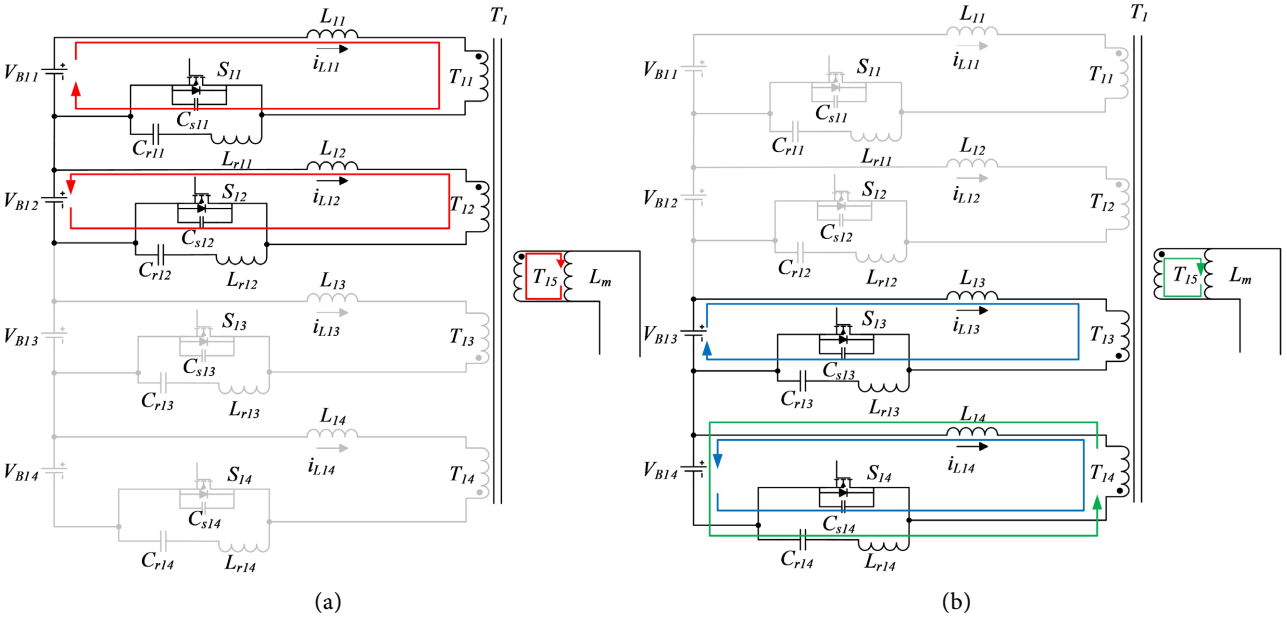

Figure 4. Battery equalization mode analysis. (a) Mode I; (b) Mode II.

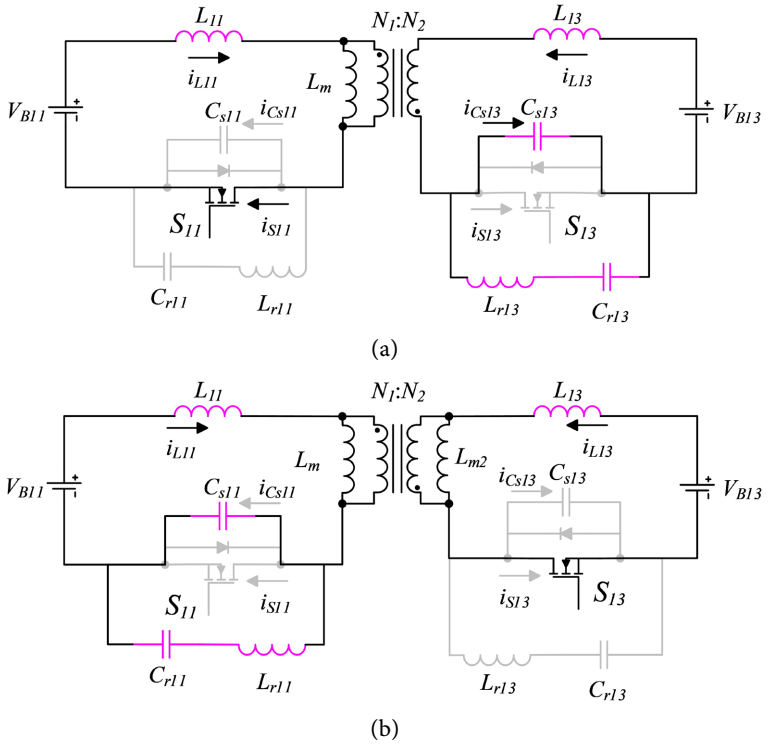

Figure 5. Parasitic elements participate in resonance. (a) Mode I; (b) Mode II.

involving C_{S13} ends when V_{CS11} falls to zero.

3. Experimental Results

Three types of experiments, as shown in Table 1, will be carried out for comparison in this research. In these experiments, a series of tests were conducted to in-

vestigate the performance of the high-frequency battery charge equalization circuit. First, a basic circuit, consisting of battery, switching elements, and transformer, is used. The resonant elements in this circuit are composed of the Miller capacitance of the parasitic switch and the leakage inductance of the transformer winding. This configuration allows observation of voltage spikes and current waveforms on the switch.

Next, an external switch bypass capacitor is connected in parallel with the Miller capacitor, to achieve circuit resonance. Finally, an *L*-*C* resonant branch is introduced to the circuit. To obtain accurate impedance values from Laplace transformation for a multi-winding converter with an added *L*-*C* resonant branch is relatively complex and challenging. Therefore, the formula in [8] is used to obtain the numerical values of the *L*-*C* resonant components. In the experiments, parameters were adjusted and designed through trial and error, and the goal of charge equalization is achieved. The system performances with high-frequency operation and different configurations are investigated and provided.

3.1. Charge Equalization without Additional Component

The experiments of charge equalization for the converter without any additional components are carried out. The switch bypass capacitance is the parasitic output capacitance of the switch, and the inductance is the leakage inductance of the winding. The measured waveforms are shown in **Figure 6**. It can be observed that there is significant interference in the Drain-Source (DS) terminal of the switch, and the transient voltage spike reaches up to 40 V.

3.2. Charge Equalization with Additional Bypass Capacitor Resonance

In the proposed circuit, in addition to the original components, an additional bypass capacitor is connected to the DS terminal of the switch. The components involved in resonance include the leakage inductance of the transformer winding, the parasitic capacitance of the switch, and the externally added bypass capacitor. The measured waveforms, shown in **Figure 7**, show that the voltage waveform on the switch exhibits a quasi-trapezoidal shape, with a peak voltage of 20 V. Although the voltage stress on the switch has been reduced, it is still unable to achieve soft-switching for all switches. The charge equalization results are shown in **Table 2**, indicating that the proposed circuit can achieve charge equalization for batteries.

Table 1. Experimental types and parameter specifications.

Experimental types	Parameter specifications
No additional component	Switch: IRLML0030TRPbF
	Battery: PHET-SP1100
	Magnetizing inductance (L_m) = 1 μH
	Leakage inductance (L_{Lk}) = 0.27 μH

Continued

Introducing switch bypass capacitor	Bypass capacitor = 1.8 nF
Implementing *L*-*C* resonance	Bypass capacitor = 1.2 nF *L* = 1.77 μH *C* = 0.47 nF

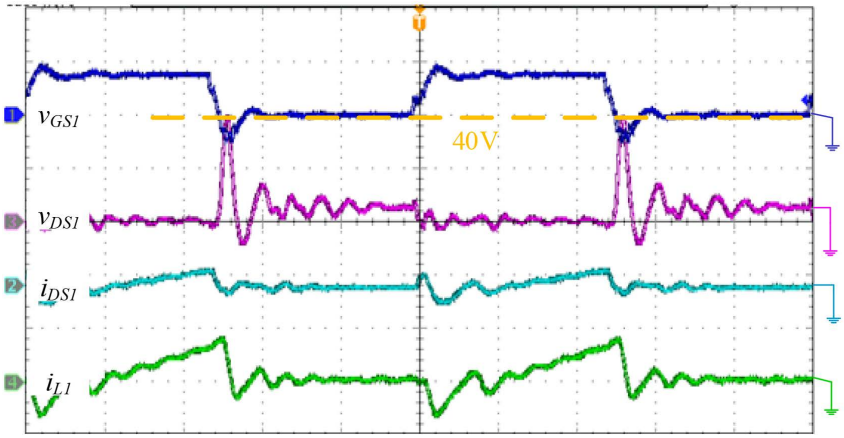

(a)

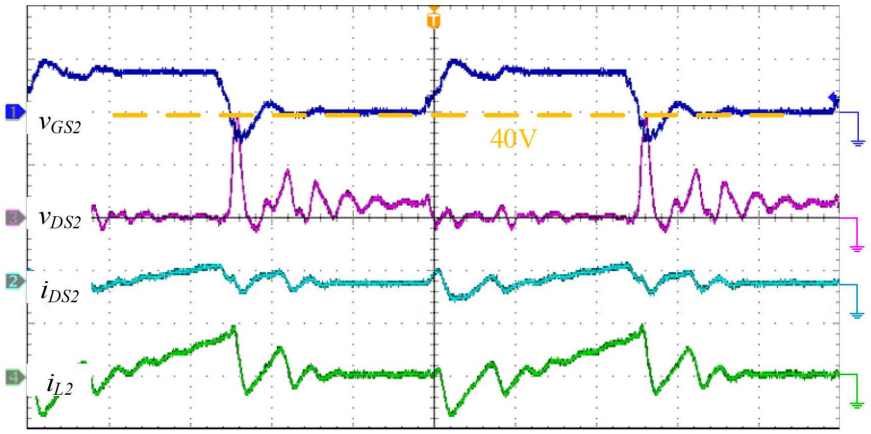

(b)

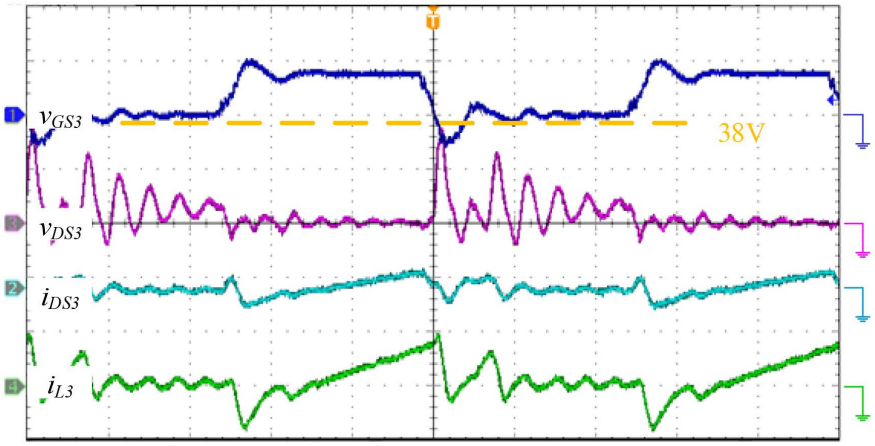

(c)

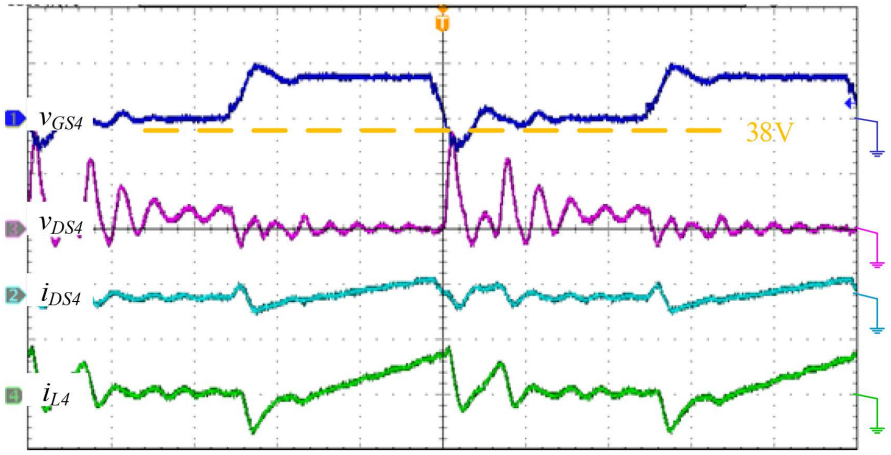

(d)

Figure 6. Charge equalization without additional component. (a) S_1; (b) S_2; (c) S_3; (d) S_4. (v_{GS}: 20 V/div, v_{DS}: 20 V/div, i_{DS}: 1 A/div, i_L: 0.5 A/div Time: 200 ns).

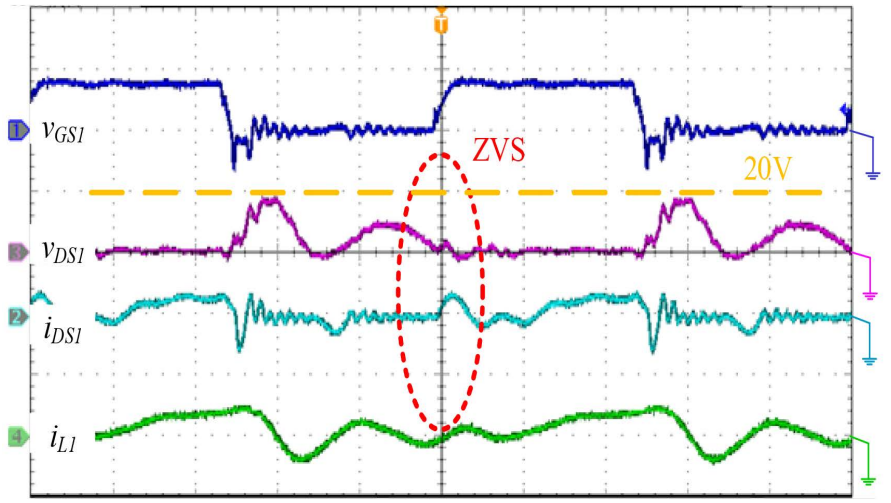

(a)

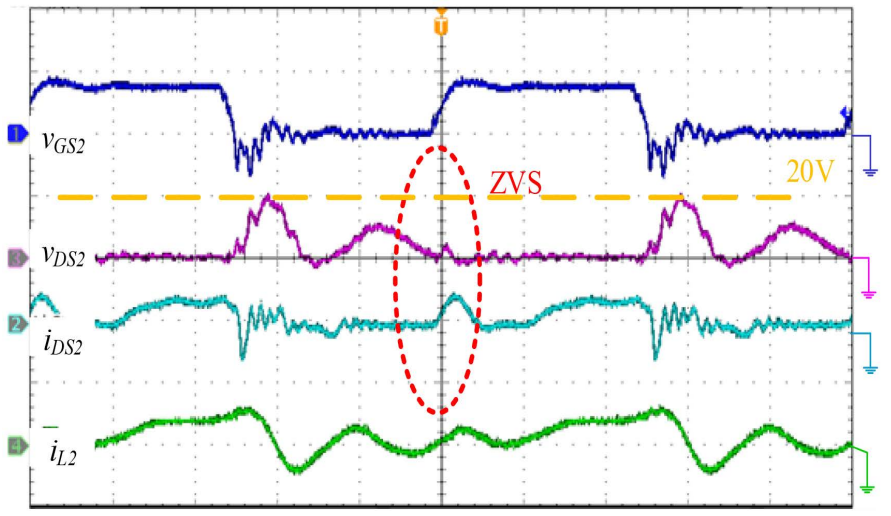

(b)

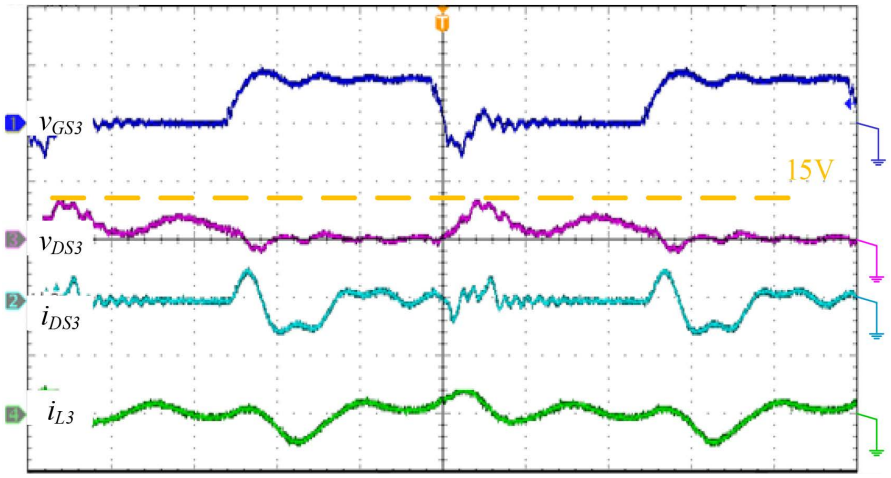

(c)

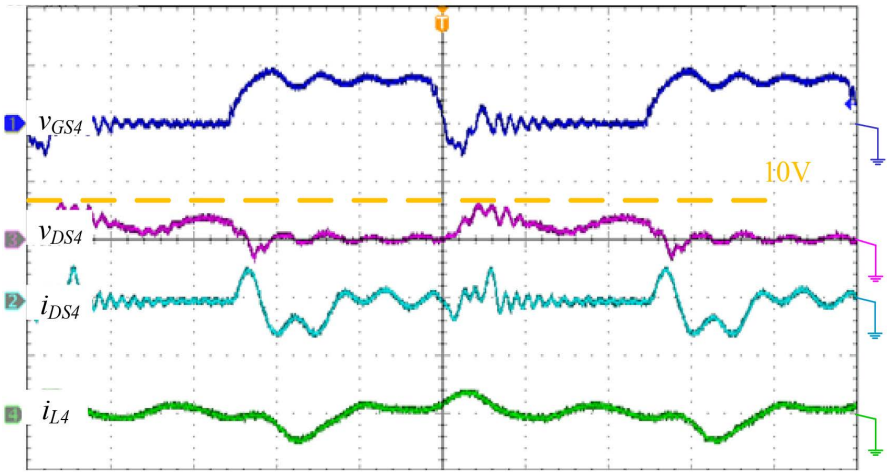

(d)

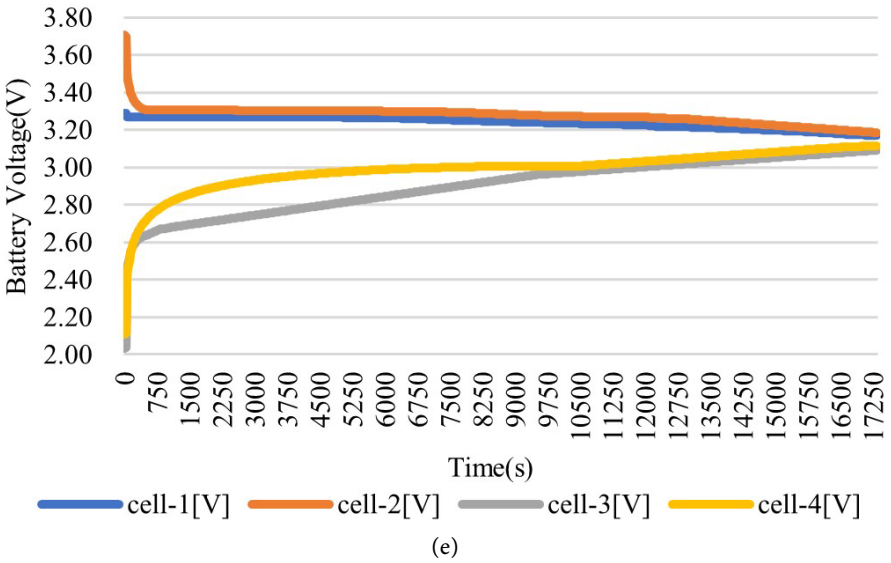

(e)

Figure 7. Charge equalization with additional bypass capacitor. (a) S_1; (b) S_2; (c) S_3; (d) S_4; (e) Battery energy balancing curve. (v_{GS}: 20 V/div, v_{DS}: 20 V/div, i_{DS}: 1 A/div, i_L: 1 A/div Time: 200 ns).

Table 2. Results of charge equalization with additional bypass capacitor resonance.

Battery number	Initial voltage (V)	Final voltage (V)
Cell 1	3.28	3.17
Cell 2	3.74	3.18
Cell 3	2.03	3.09
Cell 4	2.10	3.11
Voltage Difference (V)	1.71	<0.1

3.3. Charge Equalization with *L-C* Resonant Branch

The resonance operation can be performed by paralleling *L-C* components across the switch terminals. The charge equalization components in this configuration include the switch bypass capacitor, transformer winding leakage inductance, and the *L-C* resonant branch, all participating in resonance. The switch waveform is shown in Figure 8. It can be observed that all switches achieve soft switching, and the maximum voltage on the switch is 20V, effectively reducing the peak voltage on the switch. The charge equalization results are shown in Table 3, indicating consistent charge equalization is achieved for the system.

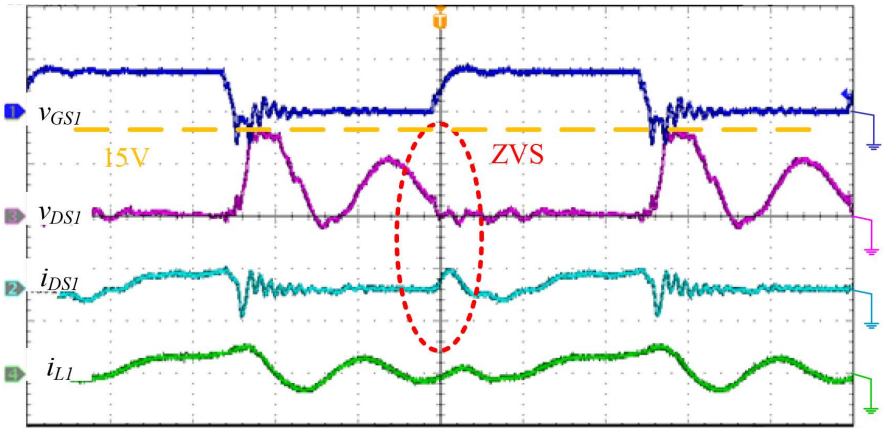

(a)

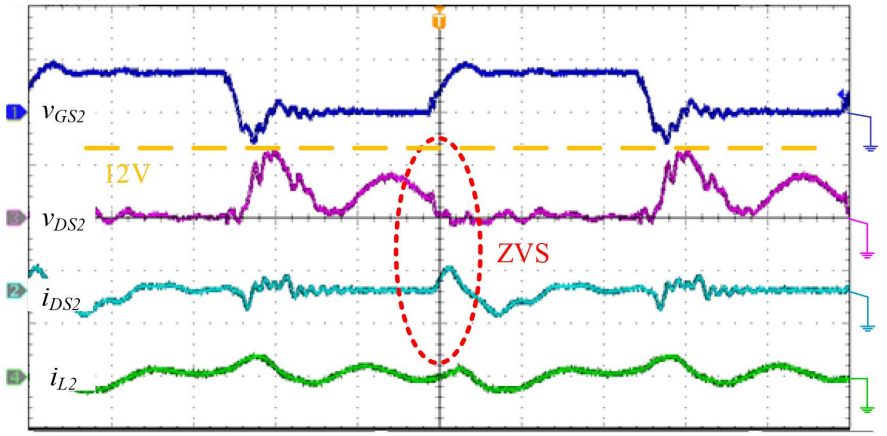

(b)

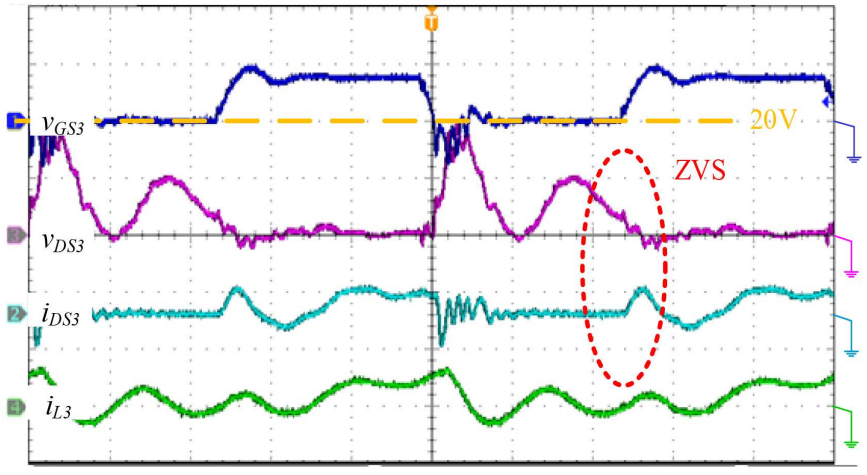

(c)

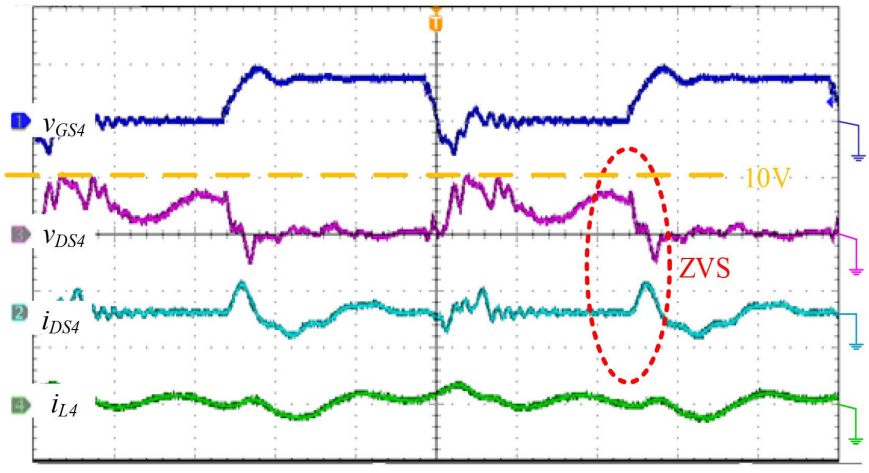

(d)

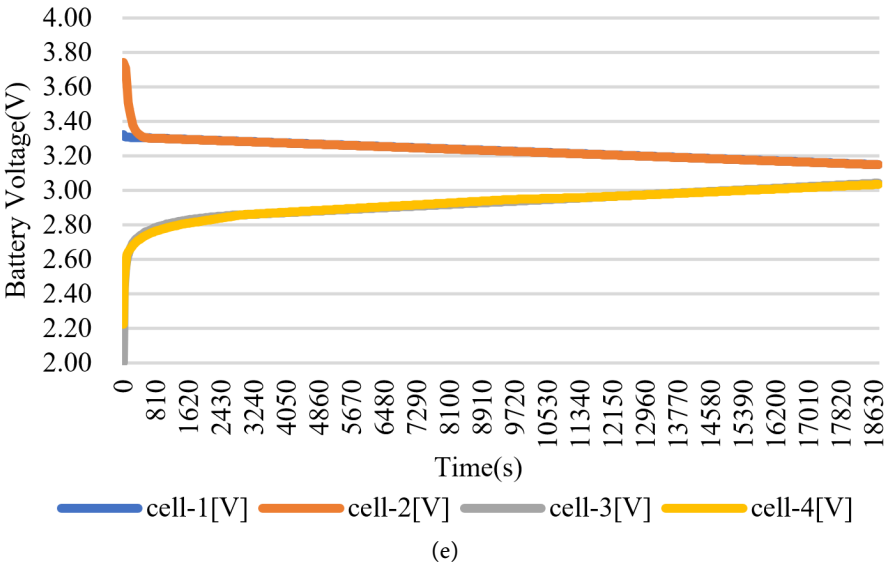

(e)

Figure 8. Charge equalization with *L-C* resonant branch. (a) S_1 (b) S_2 (c) S_3 (d) S_4 (e) Battery energy balancing curve. (v_{GS}: 20 V/div, v_{DS}: 20 V/div, i_{DS}: 1 A/div, i_L: 1 A/div Time: 200 ns).

Table 3. Results of charge equalization with *L-C* resonant branch resonance.

Battery number	Initial voltage (V)	Final voltage (V)
Cell 1	3.32	3.15
Cell 2	3.74	3.15
Cell 3	2.00	3.04
Cell 4	2.22	3.04
Voltage Difference (V)	1.74	<0.1

4. Conclusion

This paper has proposed a battery equalizer for evaluating the feasibility of achieving high frequency switching operation in battery energy applications. The main objective of this research is to increase switching frequency, reduce system cost, enhance soft-switching performance, and achieve battery charge equalization for the battery system with a lot of batteries. The proposed equalizer has the potential for development in applications for electric vehicles and energy storage systems. Experimental results show that using a bypass capacitor or an *L-C* resonant branch for the converter, the voltage spike on the switch is significantly reduced, and ZVS for the switch is achieved. The performance of the proposed converter is verified by the experimental measurements.

Conflicts of Interest

The authors declare no conflicts of interest regarding the publication of this paper.

References

[1] Li, Y., Xu, J., Mei, X. and Wang, J. (2019) A Unitized Multiwinding Transformer-Based Equalization Method for Series-Connected Battery Strings. *IEEE Transactions on Power Electronics*, **34**, 11981-11989. https://doi.org/10.1109/tpel.2019.2910205

[2] Maharjan, L., Inoue, S., Akagi, H. and Asakura, J. (2009) State-of-Charge (SOC)-Balancing Control of a Battery Energy Storage System Based on a Cascade PWM Converter. *IEEE Transactions on Power Electronics*, **24**, 1628-1636. https://doi.org/10.1109/tpel.2009.2014868

[3] Dogger, J.D., Roossien, B. and Nieuwenhout, F.D.J. (2011) Characterization of Li-Ion Batteries for Intelligent Management of Distributed Grid-Connected Storage. *IEEE Transactions on Energy Conversion*, **26**, 256-263. https://doi.org/10.1109/tec.2009.2032579

[4] Al-Haj Hussein, A. and Batarseh, I. (2011) A Review of Charging Algorithms for Nickel and Lithium Battery Chargers. *IEEE Transactions on Vehicular Technology*, **60**, 830-838. https://doi.org/10.1109/tvt.2011.2106527

[5] Roscher, M.A., Assfalg, J. and Bohlen, O.S. (2011) Detection of Utilizable Capacity Deterioration in Battery Systems. *IEEE Transactions on Vehicular Technology*, **60**, 98-103. https://doi.org/10.1109/tvt.2010.2090370

[6] Manenti, A., Abba, A., Merati, A., Savaresi, S.M. and Geraci, A. (2011) A New BMS Architecture Based on Cell Redundancy. *IEEE Transactions on Industrial Electronics*, **58**, 4314-4322. https://doi.org/10.1109/tie.2010.2095398

[7] Liu, Y., Hsieh, C. and Luo, Y. (2011) Search for an Optimal Five-Step Charging Pattern for Li-Ion Batteries Using Consecutive Orthogonal Arrays. *IEEE Transactions on Energy Conversion*, **26**, 654-661. https://doi.org/10.1109/tec.2010.2103077

[8] Kelkar, A., Dasari, Y. and Williamson, S. (2020) A Comprehensive Review of Power Electronics Enabled Active Battery Cell Balancing for Smart Energy Management. 2020 *IEEE International Conference on Power Electronics, Smart Grid and Renewable Energy* (*PESGRE*2020), Cochin, 2-4 January 2020, 1-6. https://doi.org/10.1109/pesgre45664.2020.9070666

[9] Abdul-jabbar, T.A., Kersten, A., Mashayekh, A., Obed, A.A., Abid, A.J. and Kuder, M. (2022) Efficient Battery Cell Balancing Methods for Low-Voltage Applications: A Review. 2022 *IEEE International Conference in Power Engineering Application* (*ICPEA*), Shah Alam, 7-8 March 2022, 1-7. https://doi.org/10.1109/icpea53519.2022.9744677

[10] Baronti, F., Roncella, R. and Saletti, R. (2014) Performance Comparison of Active Balancing Techniques for Lithium-Ion Batteries. *Journal of Power Sources*, **267**, 603-609. https://doi.org/10.1016/j.jpowsour.2014.05.007

[11] Ghaeminezhad, N., Ouyang, Q., Hu, X., Xu, G. and Wang, Z. (2021) Active Cell Equalization Topologies Analysis for Battery Packs: A Systematic Review. *IEEE Transactions on Power Electronics*, **36**, 9119-9135. https://doi.org/10.1109/tpel.2021.3052163

[12] Park, H.-S., *et al*. (2009) A Modularized Charge Equalizer for an HEV Lithium-Ion Battery String. *IEEE Transactions on Industrial Electronics*, **56**, 1464-1476. https://doi.org/10.1109/tie.2009.2012456

[13] Park, H.-S., *et al*. (2009) Design of a Charge Equalizer Based on Battery Modularization. *IEEE Transactions on Vehicular Technology*, **58**, 3216-3223. https://doi.org/10.1109/tvt.2009.2015331

[14] Kutkut, N.H. (1998) A Modular Nondissipative Current Diverter for EV Battery Charge Equalization. *APEC*'98 *Thirteenth Annual Applied Power Electronics Conference and Exposition*, Anaheim, 15-19 February 1998, 686-690. https://doi.org/10.1109/apec.1998.653973

[15] Kutkut, N.H. (1972) Nondissipative Current Diverter Using a Centralized Multi-Winding Transformer. PESC97. *Record* 28*th Annual IEEE Power Electronics Specialists Conference. Formerly Power Conditioning Specialists Conference* 1970-71. *Power Processing and Electronic Specialists Conference* 1972, St. Louis, 648-654. https://doi.org/10.1109/pesc.1997.616790

[16] Xu, A.G., Xie, S.J. and Liu, X.B. (2009) Dynamic Voltage Equalization for Series-Connected Ultracapacitors in EV/HEV Applications. *IEEE Transactions on Vehicular Technology*, **58**, 3981-3987. https://doi.org/10.1109/tvt.2009.2028148

[17] Uno, M. and Tanaka, K. (2011) Influence of High-Frequency Charge-Discharge Cycling Induced by Cell Voltage Equalizers on the Life Performance of Lithium-Ion Cells. *IEEE Transactions on Vehicular Technology*, **60**, 1505-1515. https://doi.org/10.1109/tvt.2011.2127500

[18] Baughman, A.C. and Ferdowsi, M. (2008) Double-Tiered Switched-Capacitor Battery Charge Equalization Technique. *IEEE Transactions on Industrial Electronics*, **55**, 2277-2285. https://doi.org/10.1109/tie.2008.918401

[19] Moo, C.S., Hsieh, Y.C. and Tsai, I.S. (2003) Charge Equalization for Series-Connected Batteries. *IEEE Transactions on Aerospace and Electronic Systems*, **39**, 704-710. https://doi.org/10.1109/taes.2003.1207276

[20] Cassani, P.A. and Williamson, S.S. (2009) Feasibility Analysis of a Novel Cell Equalizer Topology for Plug-In Hybrid Electric Vehicle Energy-Storage Systems. *IEEE Transactions on Vehicular Technology*, **58**, 3938-3946. https://doi.org/10.1109/tvt.2009.2031553

[21] Einhorn, M., Roessler, W. and Fleig, J. (2011) Improved Performance of Serially Connected Li-Ion Batteries with Active Cell Balancing in Electric Vehicles. *IEEE Transactions on Vehicular Technology*, **60**, 2448-2457. https://doi.org/10.1109/tvt.2011.2153886

[22] Kutkut, N.H., Divan, D.M. and Novotny, D.W. (1995) Charge Equalization for Series Connected Battery Strings. *IEEE Transactions on Industry Applications*, **31**, 562-568. https://doi.org/10.1109/28.382117

[23] Kutkut, N.H., Wiegman, H.L.N., Divan, D.M. and Novotny, D.W. (1999) Design Considerations for Charge Equalization of an Electric Vehicle Battery System. *IEEE Transactions on Industry Applications*, **35**, 28-35. https://doi.org/10.1109/28.740842

[24] Shang, Y., Xia, B., Zhang, C., Cui, N., Yang, J. and Mi, C. (2017) An Automatic Battery Equalizer Based on Forward and Flyback Conversion for Series-Connected Battery Strings. 2017 *IEEE Applied Power Electronics Conference and Exposition* (*APEC*), Tampa, 26-30 March 2017, 3218-3222. https://doi.org/10.1109/apec.2017.7931157

[25] Wei, Z., Peng, F. and Wang, H. (2021) An LCC Based String-to-Cell Battery Equalizer with Simplified Constant Current Control. *IEEE Transactions on Power Electronics*, **37**, 1816-1827. https://doi.org/10.1109/tpel.2021.3102627

[26] Shang, Y., Zhao, S., Fu, Y., Han, B., Hu, P. and Mi, C.C. (2020) A Lithium-Ion Battery Balancing Circuit Based on Synchronous Rectification. *IEEE Transactions on Power Electronics*, **35**, 1637-1648. https://doi.org/10.1109/tpel.2019.2917390

[27] Hsieh, Y., Wu, J. and Chen, X. (2012) Class-*e*- Based Charge-Equalisation Circuit for Battery Cells. *IET Power Electronics*, **5**, 978-983. https://doi.org/10.1049/iet-pel.2012.0073

[28] Gottwald, T., Ye, Z. and Stuart, T. (1997) Equalization of EV and HEV Batteries with a Ramp Converter. *IEEE Transactions on Aerospace and Electronic Systems*, **33**, 307-312. https://doi.org/10.1109/7.570791

[29] Kim, C., Kim, M. and Moon, G. (2013) A Modularized Charge Equalizer Using a Battery Monitoring IC for Series-Connected Li-Ion Battery Strings in Electric Vehicles. *IEEE Transactions on Power Electronics*, **28**, 3779-3787. https://doi.org/10.1109/tpel.2012.2227810

[30] Gu, L. and Zhu, W. (2021) A Family of Zero-Voltage-Switched Resonant Converters: Derivation, Operation, and Design. *IEEE Journal of Emerging and Selected Topics in Power Electronics*, **9**, 2098-2108. https://doi.org/10.1109/jestpe.2020.2978239

[31] Guan, Y., Hu, X., Zhang, S., Wang, Y., Xu, D. and Wang, W. (2019) A Novel Single Switch High-Frequency DC/DC Converter and Its Mathematical Model. *IEEE Transactions on Industry Applications*, **55**, 3877-3888. https://doi.org/10.1109/tia.2019.2901637

[32] Chung, E., Lee, K., Han, Y. and Ha, J. (2017) Single-Switch High-Frequency DC-DC Converter Using Parasitic Components. *IEEE Transactions on Power Electronics*, **32**, 3651-3661. https://doi.org/10.1109/tpel.2016.2582831